PRAMANA
— journal of
physics

Vol. 74, No. 4
April 2010
pp. 563–574

Measurement of the bremsstrahlung spectra generated from thick targets with Z=2–78 under the impact of 10 keV electrons

NAMITA YADAV, PRAGYA BHATT, RAJ SINGH,
V S SUBRAHMANYAM and R SHANKER*
Department of Physics, Atomic Physics Laboratory, Banaras Hindu University,
Varanasi 221 005, India
*Corresponding author. E-mail: shankerorama@gmail.com

MS received 26 March 2009; revised 21 October 2009; accepted 24 November 2009

Abstract. We present new experimental data on thick target bremsstrahlung spectra generated from the interaction of energetic electrons with bulk matter. The 'photon yields' in terms of double differential cross-sections (DDCS) are measured for pure elements of thick targets: Ti ($Z = 22$), Ag ($Z = 47$), W ($Z = 74$) and Pt ($Z = 78$) under the impact of 10 keV electrons. Comparison of DDCS obtained from the experimental data is made with those predicted by Monte-Carlo (MC) calculations using PENELOPE code. A close agreement between the experimental data and the MC calculations is found for all the four targets within the experimental error of 16%. Furthermore, the ratios of DDCS of bremsstrahlung photons emitted from Ag, W and Pt with those from Ti as a function of photon energy are examined with a relatively lower uncertainty of about 10% and they are compared with MC calculations. A satisfactory agreement is found between the experiment and the calculations within some normalizing factors. The variations of DDCS as a function of Z and of photon energy are also studied which show that the DDCS vary closely with Z; however, some deviations are observed for 'tip' photons emitted from high Z targets.

Keywords. Thick target bremsstrahlung photons; solid-state effects; double differential cross-sections; Monte-Carlo simulation.

PACS Nos 34.80.-i; 78.70.-g; 33.20.Rm; 34.50.Bw

1. Introduction

The impact of energetic electrons on solid targets generally produces spectra comprising of a continuous radiation aptly called the bremsstrahlung (braking-rays) spectrum along with the characteristic X-rays of the bombarded target. An energetic electron when comes under the influence of nuclear field of the target atom, accelerates or decelerates and then scatters elastically due to Coulombic interaction. This process generates the bremsstrahlung photons. It is indeed a complex

process as it involves multiple scattering events with the target atoms; several other reaction channels like, photon attenuation, electron energy loss, electron backscattering etc. come into play and they consequently affect the bremsstrahlung emission cross-sections. Bremsstrahlung radiations are involved in a variety of fields, such as, in plasma physics, radiation physics (secondary electron effects, condensed phase spur formation), astrophysics (aurora borealis, planetary atmosphere, supernova activity) and in nuclear radiation transport, shielding and dosimetry.

In the past few years, a considerable amount of experimental work has been done on bremsstrahlung cross-section measurements and many theories have been given for thin targets (single electron–atom collision). Koch and Motz [1] in 1959, presented a paper in which the bremsstrahlung cross-section formulas and related data were given. In their paper they gave emphasis to the Born approximation formulas and included various theoretical and empirical corrections to these formulas. Placious [2] produced experimental data for incident electrons having energies between 50 and 100 keV with the targets having $Z = 13$, 50 and 79 over a wide range of target thickness. Chervenak and Liuzzi [3] performed experiment on bremsstrahlung spectra in the electron energy range 10–30 keV and showed angular distributions of emitted photons. Quarles and Heroy [4] reported the double differential cross-sections (DDCS) for atomic field bremsstrahlung (AFB) photons emitted from 50, 100 and 140 keV electrons incident on thin targets of Al, Ag, Cu and Au. They compared these results with the results of Pratt *et al* [5]. Semaan and Quarles [6] published a paper on AFB for Hg ($Z = 80$) and for some rare gases and compared the results with the results of Pratt *et al* [5]. Ambrose *et al* [7] reported a work on AFB cross-sections for incident electrons with energies from 50 to 100 keV for thin targets having atomic numbers $Z = 6$–92. They compared the double differential cross-sections of bremsstrahlung with the theoretical calculations of Kissel *et al* [8] for 50, 75 and 100 keV electrons. Kleinpoppen and his coworkers [9,10] published papers on energy and angular distribution on characteristic and bremsstrahlung cross-sections produced by electron bombardment (energy range 2.5–15 keV) on free atoms (Ar, Kr, Xe). Hippler *et al* [11] investigated the Z-dependence of bremsstrahlung cross-section ($\mathrm{d}\sigma/\mathrm{d}k$) for the electron bombardment on free atoms (He, Ne, Ar, Kr, Xe, N_2 and UF_6) at low incident energies $T = 2.5$–10 keV. Goel and Shanker [12] measured the DDCS for bremsstrahlung spectra produced by 7 keV electrons incident on semi-thick targets of Ag and Au. The experimental results were compared with the results of Kissel *et al* [8]. Semaan and Quarles [13] proposed a model for calculating the thick target bremsstrahlung cross-sections for incident electrons having energies between 10 and 25 keV, corrected for electron energy loss, electron backscattering, photon attenuation in the target and efficiency of X-ray detector. Recently, Agnihotri *et al* [14] published their work on thick target bremsstrahlung emitted from 10–28 keV electrons incident on Ti, W and Pt and reported results for bremsstrahlung yield, integrated yield and mean energy of the bremsstrahlung beam. A good agreement was obtained between their experiment and MC calculations using PENELOPE code [15]. Also, the Monte-Carlo calculations are made for bremsstrahlung emission from thick tungsten target for high electron impact energies (50–500 keV) by Berger and Motz [16].

From the above, it is realized that a considerable amount of information is now available on electron bremsstrahlung process. Accurate predictions on 'thick-target'

electron bremsstrahlung production are, however, difficult to make especially in low-energy region where the kinetic energy of electrons is only a few keV.

The basic objective of this work is to test the validity and strength of the predictions of PENELOPE simulation to our experimental data with regard to the relative shape of the DDCS (or photon yields) function, DDCS ratio of bremsstrahlung emission from the considered thick targets with Ti with a reduced uncertainty and to the variation of DDCS as a function of Z and photon energy. For this, we have measured the DDCS of bremsstrahlung emission cross-sections differential in photon energy as well as in emission angle for 10 keV electrons incident on pure elements of thick targets of Ti ($Z = 22$), Ag ($Z = 47$), W ($Z = 74$) and Pt ($Z = 78$). It is demonstrated that the DDCS of bremsstrahlung emission from thick targets vary closely with Z [17]. In the analysis of the experimental data, all the 'solid-state effects' as described in §§3 and 4, are considered and their respective contributions are accounted for. The derived results for different comparisons are reported and discussed in §5.

2. Experimental details

The experiment was carried out on the experimental set-up developed in our laboratory, the details of which are given elsewhere [18,19]. A schematic diagram of the present experimental set-up is shown in figure 1. Briefly, a monoenergetic beam of 10 keV electrons extracted from a custom-built electron gun was made to fall upon highly polished, high purity (99.99%) thick targets (Ti: 0.13 mm, Ag: 0.1 mm, W: 0.5 mm, Pt: 0.1 mm) mounted on an Al-target holder. The latter was positioned in a vertical plane at the centre of the scattering chamber. The incident beam was focussed to a spot size of about 3 mm normally onto the desired target. Provision was made to monitor the target current by using a picoammeter (pA). The incident beam current was monitored on a negatively biased Faraday cup in target-out position. However, the beam current on the target was measured by integrating the charge using ORTEC model 419. The base pressure inside the scattering chamber was maintained at better than 1.6×10^{-6} Torr using two turbomolecular pumps (240 l/s and 60 l/s) backed by their respective fore pumps. The emitted bremsstrahlung photons were detected by a Si-PIN photodiode detector (M/s Amptektron Inc., USA) placed at angle $\theta = 135^\circ$ to the incident beam direction and positioned at a distance of 70 mm from the target. The photons were detected through an aperture $\Phi = 3$ mm placed in front of the detector. The aperture was covered with a 6μ hostaphan foil. The spectra were recorded on a PC-based PCA3 multichannel analyzer (M/s Oxford Instruments, USA) in a pulse height analysis (PHA) mode. The X-ray photons were also recorded with beam without target for each run; this was needed for background subtraction in the data analysis. A typical data acquisition time varied between 1 and 2 h with a beam current of less than 1 nA.

The systematic error in the measurements is about 16%, which arises due to errors in different parameters measured in the experiment. Errors in photon counting statistics are estimated to be 3.5%, beam energy ∼1%, beam integration ∼2% and detector efficiency ∼16%. The large error in detector efficiency arises due to the error involved in the measurement of the solid angle.

3. Theoretical formulations

3.1 *Double differential cross-sections*

Double differential cross-sections are calculated using the relation

$$\frac{\mathrm{d}^2\sigma}{\mathrm{d}k\,\mathrm{d}\Omega} = \frac{N_\mathrm{B}(k)}{N_\mathrm{e}N_\mathrm{t}\Delta k\Delta\Omega\varepsilon(k)}, \tag{1}$$

where $N_\mathrm{B}(k)$ is the number of bremsstrahlung photons in the photon energy interval k and $k + \mathrm{d}k$, N_e is the total number of electrons incident on the target corrected for backscattering events, N_t is the number of target atoms per cm^2, Δk is the detector resolution, $\Delta\Omega$ is the solid angle subtended by the detector at the target and $\varepsilon(k)$ is the intrinsic efficiency of the photon detector at photon energy k.

In the present measurements of Ne, the contribution of secondary electrons to the total beam current on the target has not been taken into account; however it is estimated to vary from about 4 to 7% as we go from Ti to Pt respectively. Due to this, the DDCS (calculated without considering the contribution of secondary electrons) are found to decrease only by 3 to 5% for the above targets. This contribution, in fact tends to bring the DDCS data more close to simulation results.

3.2 *Correction for backscattered electrons*

The fraction of incident electrons which come out of the target surface is termed as the backscattering coefficient η and since the average angular deviation in an elastic collision increases with Z, so does the backscattering coefficient. It is, however, found to be weakly dependent on the incident electron energy E_0. The average electron backscattering correction is given [20] as

$$R(E_0, k) = \frac{1 - \eta(E_0, Z)}{1 - \eta(E_0, Z)(k/E_0)^2}, \tag{2}$$

where $\eta(E_0, Z)$ is the backscattering coefficient taken from [21,22] and it is a function of the impact energy E_0 and the target atomic number Z. In the present work, the estimated corrections in the number of electrons due to backscattering events were found to vary from 24 to 44% as we go from Ti to Pt target respectively.

3.3 *Target thickness*

Target thickness (number of target atoms/cm^2) is calculated using the relation

$$N_\mathrm{t} = \frac{\rho N_\mathrm{A} x}{M(\mathrm{a.m.u.})}, \tag{3}$$

where ρ is the density of target element, N_{A} is the Avogadro's number, M is the mass of the target in a.m.u. and x is the maximum penetration depth for 10 keV electrons inside the target.

Maximum penetration depth x is calculated by considering the fact that the inelastic scattering of an incident electron by the target atom causes the primary electron to lose its energy by excitation and ionization of the target atom. Consequently, it slows down as it progresses through the target until eventually it reaches the Fermi level of the target and finally flows from specimen to earth. Using continuously slowing down approximation of Bethe and Ashkin [23], the stopping power or rate of loss of energy per unit path length is given by

$$-\frac{\mathrm{d}E}{\mathrm{d}x} = 78500\frac{Z\rho}{AE_0}\ln\left(1.166\frac{E_0}{J}\right), \tag{4}$$

where Z is the atomic number of the target, A is the atomic mass in a.m.u., ρ is the density of target (g/cm^3), E_0 is the incident electron energy and J is the mean ionization energy of the target atom [24], which is roughly equal to $13.5Z$ (eV).

Integration of the reciprocal of $\mathrm{d}E/\mathrm{d}x$ over the entire energy range gives the penetration depth

$$x = \int_0^{E_0} \frac{1}{(\mathrm{d}E/\mathrm{d}x)}\mathrm{d}E. \tag{5}$$

The penetration depths of 10 keV electrons in Ti, Ag, W and Pt targets are found to be 1.675×10^{-4} cm, 9.565×10^{-5} cm, 6.674×10^{-5} cm and 6.192×10^{-5} cm respectively.

3.4 *Detection efficiency*

The detection efficiency of Si-PIN diode detector is modelled by [20]

$$\begin{aligned}\varepsilon(k) = &\{1 - 0.69k^{-2.76}\} \\ &\times[\exp\{-1.86t_{\mathrm{Be}}k^{-2.9} - 0.88t_{\mathrm{h}}k^{-3.55} - 37.96t_{\mathrm{tar}}k^{-2.52}\}],\end{aligned} \tag{6}$$

where k is the emitted photon energy, t_{Be} is the thickness of beryllium window, t_{h} is the thickness of hostaphan foil and t_{tar} is the maximum penetration depth of the electrons inside the target. All these thicknesses are taken in g/cm^2.

3.5 *DDCS from Monte-Carlo simulation*

For calculating the double differential cross-sections from the results of Monte-Carlo simulation, we have divided the bremsstrahlung photon yields [14] given by the expression

$$\frac{\mathrm{d}S}{\mathrm{d}E} = \frac{\mathrm{d}^2N_{\mathrm{B}}}{N_{\mathrm{e}}\mathrm{d}\Omega\,\mathrm{d}k\varepsilon(k)}$$

by the number of target atoms N_{t} in accordance with eq. (1).

The yields of bremsstrahlung photons emitted from the considered thick targets under the impact of 10 keV electrons were calculated using the Monte-Carlo simulation code PENELOPE [15]. In the calculations, the interaction mechanisms for electrons with the target are considered as elastic scattering, inelastic scattering, innershell ionization and bremsstrahlung emission. The interaction mechanisms of emitted photons with the specimen are considered to be coherent (Rayleigh) scattering, incoherent (Compton) scattering and photoelectric absorption. The MC code simulates the transport of primary as well as secondary particles (secondary electrons and photons) and their descendents. Simulations were normalized to one incident electron to make them comparable with experimental data. The response of the detector was accounted for by convoluting the simulated spectra with a Gaussian distribution with an energy-dependent full-width at half-maximum, where dependence on photon energy was estimated by measuring X-ray spectra for different pure elements. The statistical uncertainties for the bremsstrahlung background radiation ranged from 5 to 10% at the 3σ level.

4. Solid-state effects

With a monoenergetic beam of electrons incident on a thick target, the spectral and angular distributions of the emitted radiation result from superposition of the following complex processes:

(i) Radiation by monoenergetic electrons incident on a thin target; this is given by the differential bremsstrahlung cross-sections (i.e. differential in photon energy k and photon emission angle θ).

(ii) Electron penetration into a semi-infinite medium: this includes (a) angular dispersion of electron velocities inside the target, (b) energy loss of the incident electron in the target, (c) backscattering of incident electrons from the target.

(iii) Absorption of photons in the target and surrounding materials.

Unfortunately, information on the above individual processes is far from complete at present. The differential bremsstrahlung cross-sections have been computed to a great accuracy now and have been compiled in a tabular form by Kissel *et al* [8]. With regard to process (iia), theories are available [25] to describe the angular distributions of electron velocities as a function of electron energy for an initially monoenergetic electron beam. The process (iib) causes the incident electrons to lose energy in the target for excitation and ionization of the target atomic electrons and the radiation which results mainly from collisions with nuclei. The very important process (iic) describes the events for which incident electrons leaving the target may produce radiation which reaches the photon detector. With regards to absorption (process iii) of the radiated photons in the target and surrounding materials, it is generally assumed that the photons of any energy are attenuated in the target in a simple exponential manner.

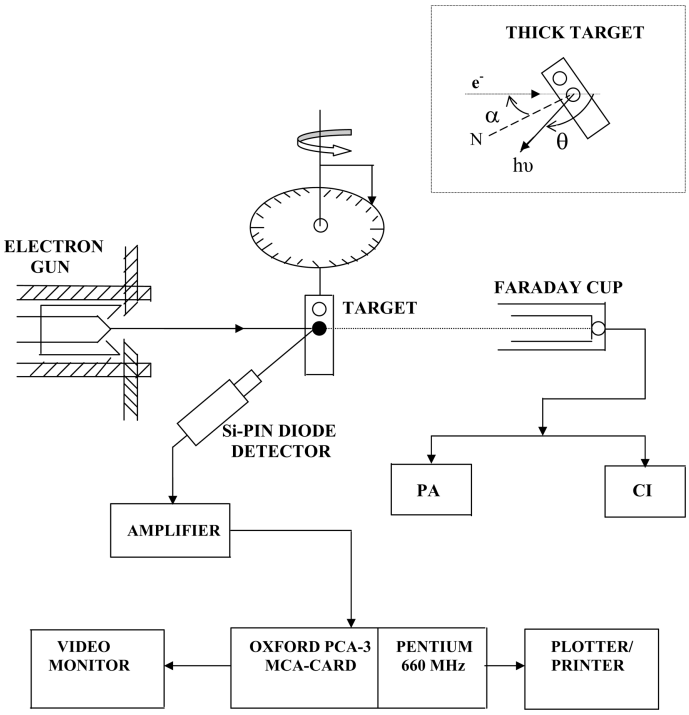

Figure 1. Schematic diagram of the experimental set-up. PA – Picoammeter; CI – current integrator. Inset shows the geometrical configuration of the detector system. α – Angle of incidence of the electron beam with respect to normal of the target (N); θ – angle of photon detection.

5. Results and discussion

5.1 *Double differential cross-sections*

The plots for the spectra of double differential cross-sections (DDCS) of bremsstrahlung radiation produced by 10 keV electrons as a function of photon energy for thick targets Ti, Ag, W and Pt are shown in figure 2. In each plot, the dashed lines and the symbols show respectively the results of MC calculation and the experimental data. The experimental data have been obtained after taking due accounts of all the above-mentioned 'solid-state effects'. The error bars on symbols represent the experimental uncertainty of about 16%.

It is noted from the plots that the DDCS decrease with photon energy. This may be due to the fact that the incident electrons entering the target lose energy continuously and consequently produce photons of continuously lower energies. The photons of all energies get absorbed by the target due to 'solid-state effects'. The 'end-point' or 'tip' photons are emitted from the elastic collisions of the incident electrons from the first few atomic layers of the target surface. The probability of emission of tip photons is quite low. Such photons are emitted from those collision

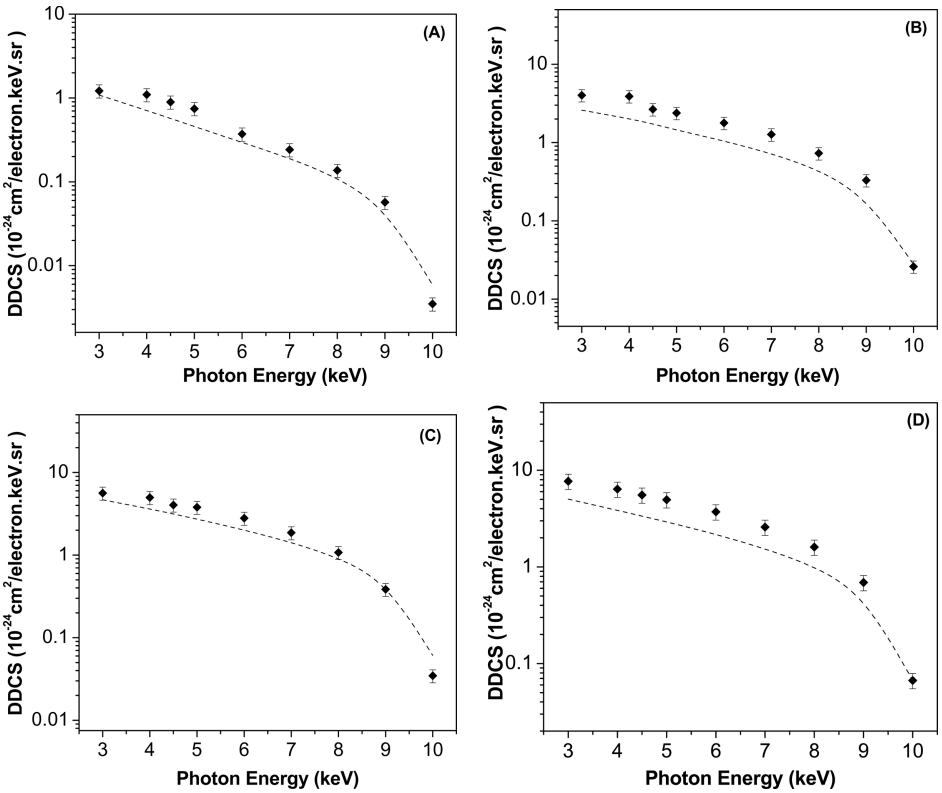

Figure 2. Plots for the spectra of DDCS of bremsstrahlung photons produced from the thick targets of : (**A**) Ti; (**B**) Ag; (**C**) W and (**D**) Pt under the impact of 10 keV electrons. The photon's detection angle with respect to incident beam direction, $\theta = 135°$. ♦: Present experiment; - - -: MC simulation.

events in which the incident electrons lose all of their energies in one encounter with the target atoms without undergoing an appreciable absorption of emitted photons by the target. This probability is expected to be maximum for elastic head-on-collision events.

The MC calculations using PENELOPE code take into account all 'solid-state effects' and their results are found to be in a reasonable agreement with experiment in the relative shape of DDCS as a function of photon energy for all the four targets (see figure 2).

5.2 *Z-dependence*

The variations of DDCS with Z of targets Ti, Ag, W and Pt for photon energies of 4.5, 6, 7, 8 and 10 keV are shown in figure 3. As seen from this figure, the values of DDCS follow the relation, DDCS$= a + bZ$, where a is seen to be negative; no plausible explanation is available at present as to why a is negative.

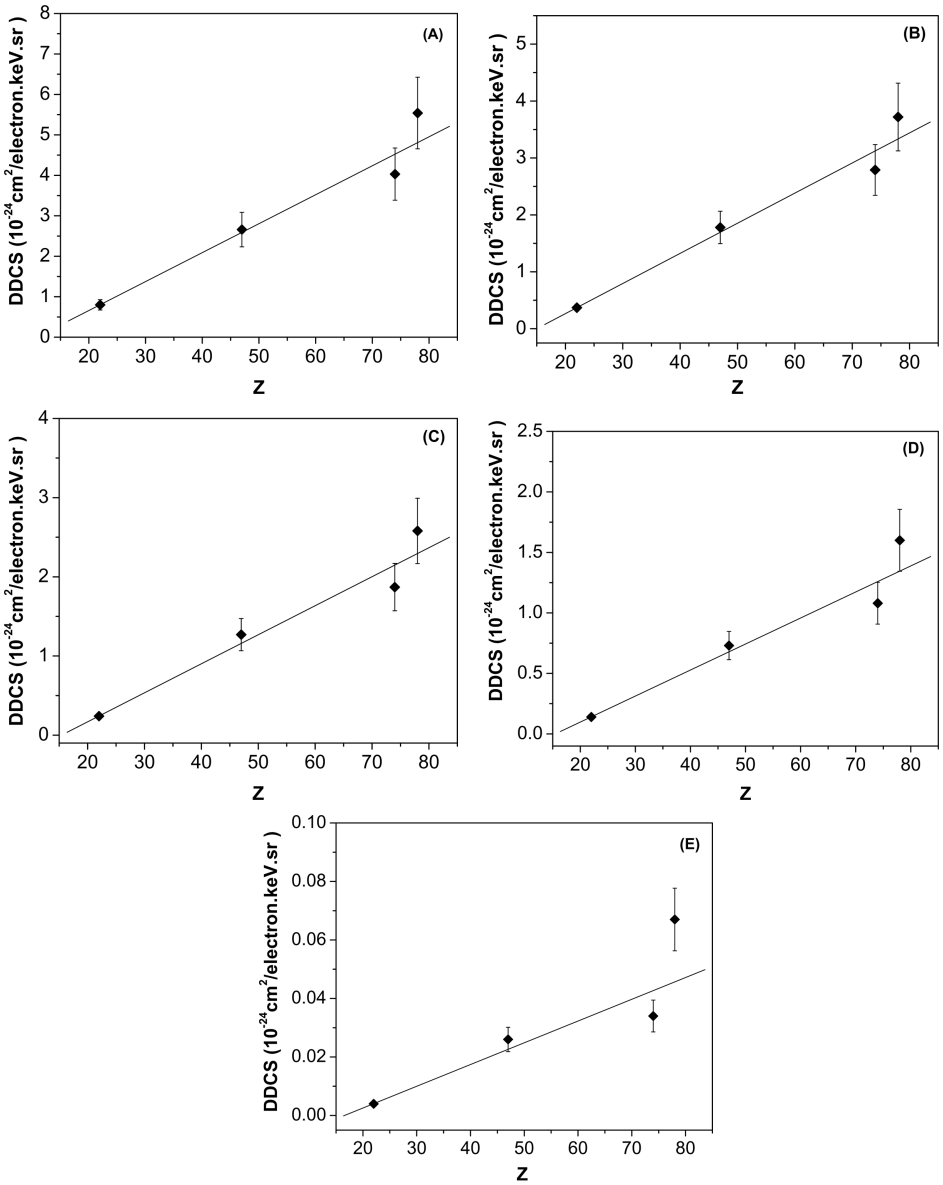

Figure 3. Variations of DDCS of bremsstrahlung photons under the impact of 10 keV electrons as a function of Z of thick targets for emission of photons at $\theta = 135^\circ$ with energy: (**A**) $k = 4.5$ keV; (**B**) $k = 6$ keV; (**C**) $k = 7$ keV; (**D**) $k = 8$ keV and (**E**) $k = 10$ keV. ♦: Present experiment; - - - : linear fit to the data points.

While going from low-energy to high-energy photon emissions, it is noted that the slope of the curve plotted between Z and DDCS goes on decreasing with photon energy. It is further noted that the high-energy photons deviate more strongly from

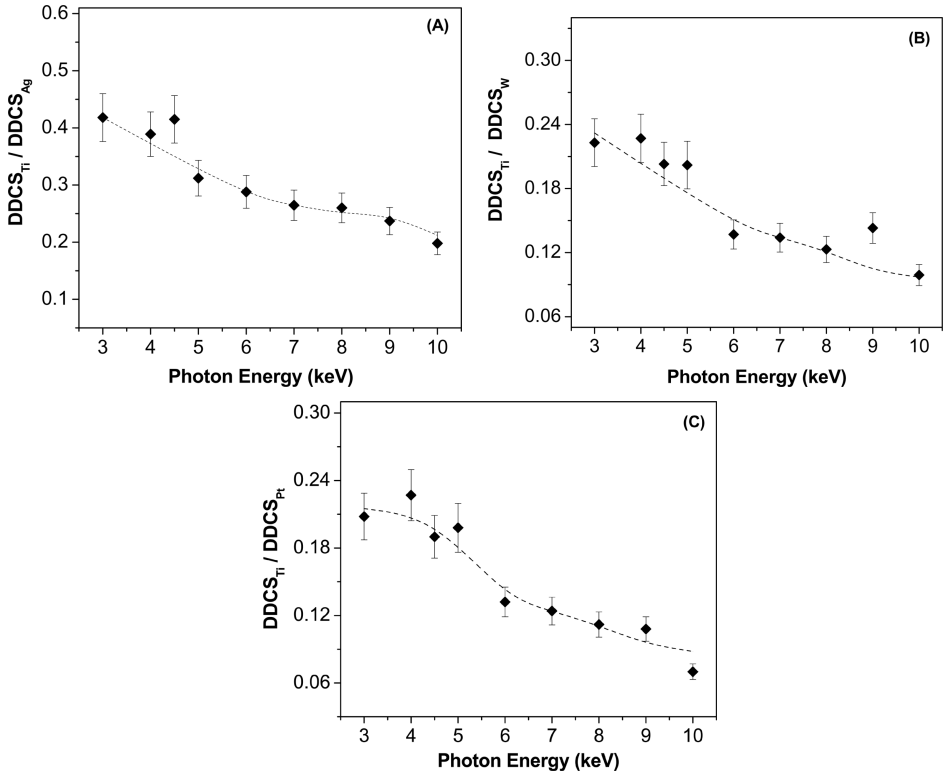

Figure 4. Ratio of DDCS of bremsstrahlung photons for: (**A**) Ti/Ag; (**B**) Ti/W and (**C**) Ti/Pt as a function of photon energy k. ♦: Present experimental data points normalized to MC calculations at $k = 7$ keV; - - - : MC calculations.

linearity than the low-energy photons; in particular, for high Z targets, for instance, the 'tip' photons. The probable reason for this deviation may be due to the fact that the high-energy photons normally come out from the upper layers of the target surface and hence a behaviour somewhat similar to 'thin target' is observed and thus the variation of DDCS with Z departs from linearity. Here, for the considered targets, the DDCS dependence on Z is seen to vary between Z (for thick target) and Z^2 (for thin target) for relatively high-energy photons.

5.3 *Double differential cross-section ratios*

Figure 4 shows the plots for ratio of DDCS of all the targets with those of titanium for an impact of 10 keV electrons. By taking the ratio of DDCS of two targets, errors arising due to solid angle, detector efficiency and energy resolution cancel out. Another advantage of taking ratio is the partial cancellation of the background due to thick target bremsstrahlung produced in the beryllium window, hostaphan foil and in the chamber walls by elastically scattered electrons. Thus the uncertainties

arising in the incident electron energy, charge collection and to a lesser extent in the background photons are the only sources of error present in the DDCS ratio. So the total experimental error reduces from 16% to about 10%.

For comparison, the experimental results are normalized with Monte-Carlo calculations at $k = 7$ keV and they are plotted in figure 4. Normalization of the experimental data with simulation aims to compare the relative shape of the double differential cross-section spectra as a function of the photon energy. The graphs presented clearly show that the experiment is in close agreement with MC calculations. The normalization factors for Ag, W and Pt are found to be 1.39, 1.03 and 1.32 respectively.

6. Conclusions

The double differential cross-sections for bremsstrahlung photons produced from 10 keV electrons incident on thick targets Ti, Ag, W and Pt are measured. The experimental data are compared with the results of Monte-Carlo simulation using the PENELOPE code. A reasonable agreement is found for DDCS between the experimental data and the MC calculations within the estimated error. In the DDCS ratio graphs, a good relative shape of experiment with MC calculations has been observed.

The Z-dependence of DDCS does not seem to be strong for photons of kinematic end point. It increases very slowly with increasing Z. A deviation from Z dependence is noticeable for 'tip' photons in particular.

To summarize, mismatches do exist between experiment and Monte-Carlo simulation. They provide, however, a rough estimate on the strengths of various 'solid-state effects', namely, multiple scattering, absorption of photons, energy loss of incident electrons and their secondaries and backscattering processes that are inherently present while the bremsstrahlung photons are emitted from thick targets under bombardment of keV electrons. These results strongly suggest the requirement for developing a comprehensive theory for understanding the emission of bremsstrahlung radiation from thick targets.

Acknowledgements

The present work was carried out with the financial support from Department of Science and Technology (DST), New Delhi under research grants Nos SR/S2/LOP-09/2006 and SR/S2/RFLOP-02/2006. The authors are thankful to Xavier Llovet (Barcelona, Spain) for performing MC calculations for the desired targets and for his valuable suggestions. Namita Yadav, Pragya Bhatt and Raj Singh thankfully acknowledge the award of research fellowships to them by DST during this work.

References

[1] H W Koch and J W Motz, *Rev. Mod. Phys.* **31**, 920 (1959)
[2] R C Placious, *J. Appl. Phys.* **38**, 2030 (1967)
[3] J G Chervenak and A Liuzzi, *Phys. Rev.* **A12**, 26 (1975)

[4] C A Quarles and D B Heroy, *Phys. Rev.* **A24**, 48 (1981)
[5] R H Pratt, H K Tseng, C M Lee, Lynn Kissel, Crawford MacCallum and Merle Riley, *At. Data Nucl. Data Tables* **20**, 175 (1977)
C M Lee, Lynn Kissel, R H Pratt and H K Tseng, *Phys. Rev.* **A13**, 1714 (1976)
H K Tseng, R H Pratt and C M Lee, *Phys. Rev.* **A19**, 187 (1979)
[6] M Semaan and C Quarles, *Phys. Rev.* **A26**, 3152 (1982)
[7] R Ambrose, J C Altman and C A Quarles, *Phys. Rev.* **A35**, 529 (1987)
[8] L Kissel, C A Quarles and R H Pratt, *At. Data Nucl. Data Tables* **28**, 381 (1983)
[9] M Aydinol, R Hippler, I McGregor and H Kleinpoppen, *J. Phys.* **B13**, 989 (1980)
[10] R Hippler, K Saeed, I McGregor and H Kleinpoppen, *Z. Phys.* **A307**, 83 (1982)
[11] R Hippler, K Saeed, I McGregor and H Kleinpoppen, *Phys. Rev. Lett.* **46**, 1622 (1981)
[12] S K Goel and R Shanker, *J. X-ray Sci. Technol.* **7**, 331 (1997)
[13] Mars Semaan and C A Quarles, *X-ray Spectrom.* **30**, 37 (2001)
[14] A N Agnihotri, V S Subrahmanyam, R K Yadav, R Shanker and X Llovet, *J. Phys. D: Appl. Phys.* **41**, 065205 (2008)
[15] F Salvat, J M Fernández-Varea and J Sempau, *PENELOPE-2006*: *A code system for Monte Carlo simulation of electron and photon transport*, 2006 (Issy les Molineaux: OECD Nuclear Energy Agency). Available in pdf format from: http://www.nea.fr/html/dbprog/penelope.pdf
[16] M J Berger and J W Motz, *Nucl. Instrum. Methods: Phys. Res.* **B226**, 327 (2004)
[17] H A Kramers, *Philos. Mag.* **46**, 836 (1923)
[18] R K Singh, R K Mohanta, R Hippler and R Shanker, *Pramana – J. Phys.* **58**, 499 (2002)
[19] R K Yadav and R Shanker, *Phys. Rev.* **A70**, 052901 (2004)
[20] R Ambrose, D L Kahler, H E Lehtihet and C A Quarles, *Nucl. Instrum. Methods: Phys. Res.* **B56**, 327 (1991)
[21] R K Yadav and R Shanker, *J. Electr. Spectr. Rel. Phen.* **151**, 71 (2006)
[22] R K Yadav, A Srivastava, S Mondal and R Shanker, *J. Phys. D: Appl. Phys.* **36**, 2538 (2003)
[23] H A Bethe and J Ashkin, *Experimental nuclear physics* (John Wiley and Sons, New York, 1953), p. 252
[24] F Bloch, *Z. Phys.* **81**, 263 (1933)
[25] S Goudsmit and J L Saunderson, *Phys. Rev.* **57,** 24 (1940)
H W Lewis, *Phys. Rev.* **78**, 526 (1950)